



This is a repository copy of *Simultaneous wireless information and power transfer based on generalized triangular decomposition*.

White Rose Research Online URL for this paper:
<https://eprints.whiterose.ac.uk/145340/>

Version: Accepted Version

Article:

Al-Baidhani, A., Vehkaperä, M. and Benaissa, M. orcid.org/0000-0001-7524-9116 (2019) Simultaneous wireless information and power transfer based on generalized triangular decomposition. *IEEE Transactions on Green Communications and Networking*, 3 (3). pp. 751-764.

<https://doi.org/10.1109/TGCN.2019.2911161>

© 2019 IEEE. Personal use of this material is permitted. Permission from IEEE must be obtained for all other users, including reprinting/ republishing this material for advertising or promotional purposes, creating new collective works for resale or redistribution to servers or lists, or reuse of any copyrighted components of this work in other works. Reproduced in accordance with the publisher's self-archiving policy.

Reuse

Items deposited in White Rose Research Online are protected by copyright, with all rights reserved unless indicated otherwise. They may be downloaded and/or printed for private study, or other acts as permitted by national copyright laws. The publisher or other rights holders may allow further reproduction and re-use of the full text version. This is indicated by the licence information on the White Rose Research Online record for the item.

Takedown

If you consider content in White Rose Research Online to be in breach of UK law, please notify us by emailing eprints@whiterose.ac.uk including the URL of the record and the reason for the withdrawal request.



eprints@whiterose.ac.uk
<https://eprints.whiterose.ac.uk/>

Simultaneous Wireless Information and Power Transfer Based on Generalized Triangular Decomposition

Ahmed Al-Baidhani, *Student Member, IEEE*, Mikko Vehkaperä, *Member, IEEE*,
and Mohammed Benaissa, *Senior Member, IEEE*

Abstract

In this paper, a new approach, based on the generalized triangular decomposition (GTD), is proposed for simultaneous wireless information and power transfer (SWIPT) in the spatial domain for a point-to-point multiple-input multiple-output (MIMO) system. The proposed approach takes advantage of the GTD structure to allow the transmitter to use the strongest eigenchannel jointly for energy harvesting and information exchange while these transmissions can be separated at the receiver. The optimal structure of the GTD that maximizes the total information rate constrained by a given power allocation and a required amount of energy harvesting is derived. An algorithm is developed that minimizes the total transmitted power for given information rate and energy harvesting constraints with a limited total power at the transmitter. Both theoretical and simulation results show that our proposed GTD based SWIPT outperforms singular value decomposition (SVD) based SWIPT. This is due to the flexibility introduced by the GTD to increase the energy harvested via interstream interference.

Index Terms

Energy harvesting, SWIPT, MIMO channel, singular value decomposition, generalized triangular decomposition, optimization.

I. INTRODUCTION

The provision of automated approaches to supply energy to wireless devices deployed in resource constrained environments is fast emerging as a key enabler to sustain current progress in

This paper was presented in part at the Tenth International Conference on Wireless Communications and Signal Processing, October 18-20, 2018, Hangzhou, China.

A.Al-Baidhani and M.Benaissa are with the Department of Electronic and Electrical Engineering, University of Sheffield, Sheffield S1 3JD, U.K. (e-mail:aaaal-baidhani1@sheffield.ac.uk; m.benaissa@sheffield.ac.uk).

M.Vehkaperä was with the Department of Electronic and Electrical Engineering, University of Sheffield, Sheffield S1 3JD, U.K. He is now with the School of Electrical Engineering, Aalto University, Espoo, Finland. (e-mail: mikko.vehkaperä@aalto.fi).

wireless applications and deliver the forecast growth in these applications. Among multiple forms of automated energy sources, electromagnetic waves of the wireless signals are considered a promising solution for energy harvesting (EH) [1]. Indeed, the energy content in electromagnetic waves can for example be converted to DC voltage by using specific rectenna circuits [2]–[5]. Wireless energy transfer can also be combined with simultaneous information transfer, a concept known as simultaneous wireless information and power transfer (SWIPT) [6].

The first information-theoretic study that considered simultaneous information transmission and power transfer was conducted by Varshney [7]. The paper characterized the trade-off between the energy harvesting and the information rate for point-to-point binary discrete and additive white Gaussian noise (AWGN) channels. This study was extended to a frequency-selective AWGN channel in [8]. Both studies assumed an ideal receiver that could decode the information and harvest the energy from the same signal, which was a practical limitation.

In [9], time-switching (TS) and power-splitting (PS) techniques were proposed to overcome this limitation; in TS, the receiver has the ability to switch between decoding information and harvesting energy while in PS, the receiver has the ability to split the received signal in two parts, one for decoding information and one for harvesting energy. Since then, SWIPT based on TS and PS techniques has been widely investigated in both single and multiuser network configurations and scenarios, such as, single- and multi-antenna relay systems [10], [11], multiuser MISO [12]–[15] and MIMO [16]–[18] networks, interference channels [19], [20] and full-duplex [21] systems. In these studies, multiple antennas at the transmitter are utilized for beamforming the transmissions towards the receiver(s), where TS or PS is used for separating the information and energy streams.

Instead of transmit-side beamforming combined with TS or PS at the receiver, a novel approach utilizing spatial switching (SS) of the information and energy was proposed in [22]. Using singular value decomposition (SVD), the point-to-point MIMO channel can be transformed into parallel channels carrying either information or energy so that neither TS nor PS is necessary. The problem of minimizing the transmitted power subject to information rate and energy harvesting constraints was solved using Lagrange optimization theory. This work was extended in [23], [24] to find jointly the optimal subchannel assignment and the optimal power allocation that minimizes the total transmit power subject to information rate, energy harvesting and instantaneous per subchannel power constraints. Two exponentially complex optimal solutions based on integer programming along with a suboptimal heuristic algorithm were proposed given either perfect or

imperfect channel knowledge. The SS concept of [22]–[24] was further studied in [25], where the problem of joint antenna selection, subchannel assignment and power allocation for maximizing the energy efficiency was investigated. Similar setup and rate constrained EH optimization via joint subchannel assignment and power allocation was later considered in [26].

The common assumption in the studies [7]–[26] is that the output power of the energy harvester is linearly proportional to its input power, that is, the EH efficiency of the rectifier is constant and independent of the input. Measurements and circuit simulations of actual rectifier implementations have shown that this is approximately true only when the rectifier input power is within a limited range that depends on the rectifier design [27]–[29]. Based on this observation, a simple parametric EH model that depends only on the received signal power was proposed in [30]. Due to its simplicity and ability to match measured EH efficiency quite well, the model has been used extensively in the recent SWIPT literature, see for example [31]–[34] and references therein. An alternative analytical model based on diode characteristics of the rectifier was proposed in [35], where it was shown that the harvested energy is in general a function of the entire received signal waveform, not just the received power. Later researches [36]–[40] have investigated the use of this model for waveform design. Even though the diode-based model is more accurate than the one proposed in [30] when the rectifier input power is low, for fixed waveform and moderate-to-high input power at the rectifier, both EH models yield comparable results [41].

A. Contribution

In this paper, we propose a novel approach for spatial domain SWIPT, in a point-to-point MIMO system, based on the generalized triangular decomposition (GTD) [42]. While GTD has been previously proposed for creating spatial subchannels with equal [43] or flexible [44] predefined information rates in MIMO communication systems, we believe the current work is the first to deploy the GTD for SWIPT. In particular, the properties of the GTD are exploited so that the transmitter can use the best subchannel jointly for energy harvesting and information exchange and the receiver can separate these transmissions. This leads to significant performance improvement over the SVD based SWIPT approach.

The key contributions¹ in the paper are summarized as follows:

¹Parts of this paper have been published in [45], where some initial results without detailed derivations for the linear EH model have been reported. In addition to a detailed exposition, the present work includes additional results, complexity analysis and an extension to the non-linear EH model.

- Development of an optimal solution for SWIPT based on GTD that minimizes the total transmitted power for given rate and energy harvesting constraints under a limited available total power at the transmitter. The results show that significant savings in the total power are achieved with the proposed method compared with those obtained by the SVD.
- Derivation of an optimal structure of the GTD for SWIPT that maximizes the total information rate for a given power allocation and energy harvesting constraint. It is shown, both theoretically (Theorem 2) and via numerical analysis, that the proposed approach well outperforms the SVD based SWIPT approach.
- The above results are derived for the simplified linear EH model. An extension of SWIPT based on GTD is presented for the non-linear EH model proposed in [30].

Notation: Lower case symbols refer to scalars while upper case and lower case bold symbols refer to matrices and vectors, respectively. Calligraphic letters refer to sets. $(\cdot)^H$ and $(\cdot)^T$, represent the conjugate transpose operation and the transpose operation, respectively. $\text{tr}(\cdot)$ and $\mathbb{E}(\cdot)$ denote to the trace operator and the expectation operator, respectively. The absolute value operator is represented by $|\cdot|$ while the norm operator is represented by $\|\cdot\|$. \mathbf{I}_N represents the identity matrix of order N . $\mathbf{A}_{(i:k,j:l)}$ represents a submatrix with elements taken from the i -th row to the k -th row and from the j -th column to l -th column of the matrix \mathbf{A} .

The paper is organized as follows: Section II is divided into three subsections: The first one introduces the GTD algorithm, the second presents the system model with linear EH model where the GTD algorithm is employed in a point-to-point MIMO system, and the last one provides an illustrative example that shows how GTD can improve the performance of SWIPT compared to SVD based solution. In Section III, an algorithm is presented for energy harvesting transceiver design that minimizes the total transmit power for SWIPT based on GTD. Section IV extends the previous results to the case of a non-linear EH model. Section V discusses and compares the results of the GTD approach against the SVD approach and Section VI concludes the paper.

II. PRELIMINARIES AND MOTIVATION

In this section, we first briefly revisit the GTD, then describe the MIMO SWIPT system model used for the rest of the paper and finally provide a motivational example which shows that GTD based SWIPT can offer higher information rate than SVD based SWIPT for a given power allocation and energy harvesting constraint. To the best of our knowledge, no work to date has considered the use of the GTD for energy harvesting.

A. Generalized Triangular Decomposition

Let us first recall the definition of multiplicative majorization and then recap [42, Theorem 2.3] that provides the necessary and sufficient conditions for GTD of a given matrix to exist.

Definition 1. (Multiplicative majorization [46]) Let $\mathbf{u} = [u_1, \dots, u_n]^T$ and $\mathbf{v} = [v_1, \dots, v_n]^T$ be two real-valued vectors with positive elements. Vector \mathbf{u} is multiplicatively majorized by \mathbf{v} if $u_1 u_2 \cdots u_n = v_1 v_2 \cdots v_n$ and their descendingly ordered elements satisfy

$$\prod_{i=1}^k u_i \leq \prod_{i=1}^k v_i, \quad (1)$$

for all $1 \leq k < n$. In the following, the terms multiplicative majorization and majorization are used interchangeably and denoted $\mathbf{u} \leq \mathbf{v}$ for brevity.

Theorem 1 (Generalized triangular decomposition [42]). Consider a matrix $\mathbf{H} \in \mathbb{C}^{m \times n}$ that has rank K and positive singular values $\boldsymbol{\sigma} = [\sigma_1, \dots, \sigma_K]$. The matrix \mathbf{H} can be decomposed as

$$\mathbf{H} = \mathbf{Q}\mathbf{R}\mathbf{X}^H, \quad (2)$$

if and only if the positive diagonal elements of \mathbf{R} are multiplicatively majorized by $\boldsymbol{\sigma}$. Matrices $\mathbf{Q} \in \mathbb{C}^{m \times m}$ and $\mathbf{X} \in \mathbb{C}^{n \times n}$ are unitary matrices (or real orthogonal matrices if \mathbf{H} is real) while $\mathbf{R} \in \mathbb{R}^{m \times n}$ is a rectangular matrix whose upper-left corner is a $K \times K$ upper triangular matrix and the rest of the elements are zeros.

The decomposition given in Theorem 1 introduces flexibility to define a vector $\mathbf{r} = [r_1, \dots, r_K]^T$ as the positive diagonal of the matrix \mathbf{R} as long as $\mathbf{r} \leq \boldsymbol{\sigma}$. In addition, some structure can be forced also on the off-diagonal elements of \mathbf{R} , as can be observed from the algorithm below that calculates the decomposition (2). For more details on GTD, see [42].

GTD Algorithm

- 1) Given the SVD of \mathbf{H} as $\mathbf{H} = \mathbf{U}\boldsymbol{\Sigma}\mathbf{V}^H$ and a prescribed vector $\mathbf{r} = [r_1, \dots, r_K]^T \in \mathbb{R}^K$ that satisfies $\mathbf{r} \leq \boldsymbol{\sigma}$, iteration $k = 1$ is initialized by setting $\mathbf{Q} = \mathbf{U}$, $\mathbf{X} = \mathbf{V}$, and $\mathbf{R} = \boldsymbol{\Sigma}$.
- 2) Indices p and q are defined as

$$p = \arg \min_{k \leq i \leq K} \{R_{ii} : R_{ii} \geq r_k\}, \quad (3a)$$

$$q = \arg \max_{k \leq i \leq K} \{R_{ii} : R_{ii} \leq r_k \wedge i \neq q\}, \quad (3b)$$

where R_{ij} denotes the (i, j) th elements of \mathbf{R} . Let $\alpha_k = R_{pp}$ and $\beta_k = R_{qq}$ for future convenience and perform the following permutations on the matrices \mathbf{R} , \mathbf{X} and \mathbf{Q} :

$$(R_{kk}, R_{k+1k+1}) \leftrightarrow (R_{pp}, R_{qq}), \quad (4a)$$

$$(\mathbf{R}_{(1:k-1,k)}, \mathbf{R}_{(1:k-1,k+1)}) \leftrightarrow (\mathbf{R}_{(1:k-1,p)}, \mathbf{R}_{(1:k-1,q)}), \quad (4b)$$

$$(\mathbf{X}_{(:,k)}, \mathbf{X}_{(:,k+1)}) \leftrightarrow (\mathbf{X}_{(:,p)}, \mathbf{X}_{(:,q)}), \quad (4c)$$

$$(\mathbf{Q}_{(:,k)}, \mathbf{Q}_{(:,k+1)}) \leftrightarrow (\mathbf{Q}_{(:,p)}, \mathbf{Q}_{(:,q)}). \quad (4d)$$

The permutations in (4a) and (4b) can also be written in matrix form $\tilde{\mathbf{R}} = \mathbf{\Pi}_2^T \mathbf{R} \mathbf{\Pi}_1$, while the expressions (4c) and (4d) are equivalent to $\tilde{\mathbf{X}} = \mathbf{X} \mathbf{\Pi}_1$ and $\tilde{\mathbf{Q}} = \mathbf{Q} \mathbf{\Pi}_2$, respectively, where $\mathbf{\Pi}_1 \in \mathbb{R}^{n \times n}$ and $\mathbf{\Pi}_2 \in \mathbb{R}^{m \times m}$ are appropriate permutation matrices.

3) Construct two matrices, \mathbf{G}_1 and \mathbf{G}_2 , as follows

$$\mathbf{G}_1 = \begin{bmatrix} c & -s \\ s & c \end{bmatrix}, \quad \mathbf{G}_2 = \frac{1}{r_k} \begin{bmatrix} c\alpha_k & -s\beta_k \\ s\beta_k & c\alpha_k \end{bmatrix}. \quad (5)$$

The variables s and c are given by $s = 0$ and $c = 1$ if $\alpha_k = \beta_k = r_k$ and

$$c = \sqrt{\frac{r_k^2 - \beta_k^2}{\alpha_k^2 - \beta_k^2}}, \quad s = \sqrt{1 - c^2}, \quad (6)$$

otherwise. Note that the matrices \mathbf{G}_1 and \mathbf{G}_2 are orthogonal. Then, let $\mathbf{B}_1 = \mathbf{I}_n$ and $\mathbf{B}_2 = \mathbf{I}_m$ and update the elements of \mathbf{B}_1 and \mathbf{B}_2 as

$$\mathbf{B}_{1(k:k+1,k:k+1)} = \mathbf{G}_1, \quad \mathbf{B}_{2(k:k+1,k:k+1)} = \mathbf{G}_2. \quad (7)$$

The matrices $\tilde{\mathbf{R}}$, $\tilde{\mathbf{X}}$ and $\tilde{\mathbf{Q}}$ are then updated to $\hat{\mathbf{R}}$, $\hat{\mathbf{X}}$ and $\hat{\mathbf{Q}}$ as follows

$$\hat{\mathbf{R}} = \mathbf{B}_2^H \tilde{\mathbf{R}} \mathbf{B}_1, \quad (8a)$$

$$\hat{\mathbf{X}} = \tilde{\mathbf{X}} \mathbf{B}_1, \quad \hat{\mathbf{Q}} = \tilde{\mathbf{Q}} \mathbf{B}_2. \quad (8b)$$

Note that (8a) ensures that the element \hat{R}_{kk} is updated to r_k . For future convenience, we also remark that according to (8a), the elements \hat{R}_{kk+1} and \hat{R}_{k+1k+1} are given by

$$\hat{R}_{kk+1} = \frac{sc(\alpha_k^2 - \beta_k^2)}{r_k}, \quad (9a)$$

$$\hat{R}_{k+1k+1} = \frac{\alpha_k \beta_k}{r_k}. \quad (9b)$$

4) While $k < K$, set $\mathbf{R} = \hat{\mathbf{R}}$, $\mathbf{X} = \hat{\mathbf{X}}$ and $\mathbf{Q} = \hat{\mathbf{Q}}$ and then replace k by $k + 1$. Go to Step 2).

5) If $k = K$, replace R_{KK} by r_K and \mathbf{H} is decomposed into \mathbf{QRX}^H based on \mathbf{r} .

We denote the outcome of this algorithm as $[\mathbf{Q}, \mathbf{R}, \mathbf{X}] \leftarrow \text{GTD}(\mathbf{H}, \mathbf{r})$ in the following sections.

Remark 1. The GTD provided by the above algorithm is related to the SVD as [42]

$$\mathbf{H} = \underbrace{\mathbf{U}(\mathbf{Q}_1 \cdots \mathbf{Q}_{K-1})}_{\mathbf{Q}} \underbrace{\mathbf{R}(\mathbf{X}_{K-1}^H \cdots \mathbf{X}_1^H)}_{\mathbf{X}^H} \mathbf{V}^H, \quad (10a)$$

$$\mathbf{R} = (\mathbf{Q}_{K-1}^H \cdots \mathbf{Q}_1^H) \underbrace{\mathbf{\Sigma}}_{\mathbf{\Sigma}} (\mathbf{X}_1 \cdots \mathbf{X}_{K-1}), \quad (10b)$$

where \mathbf{Q}_k and \mathbf{X}_k are the matrices created in Step 4) during iteration $k = 1, \dots, K - 1$. The direct implication of (10) is that the matrix \mathbf{R} is obtained from $\mathbf{\Sigma}$ through a series of rotations by unitary matrices so that the energy $\text{tr}(\mathbf{\Sigma}\mathbf{\Sigma}^H) = \text{tr}(\mathbf{R}\mathbf{R}^H)$ is conserved.

B. System Model

Consider a point-to-point MIMO system where the source and the destination are equipped with N_t and N_r antennas, respectively. The transmitter uses a linear precoder to transmit information and energy simultaneously and the destination applies a linear filter on the received signal to harvest energy and to decode information in the spatial domain. Narrowband transmission over a flat fading MIMO channel represented by a complex matrix $\mathbf{H} \in \mathbb{C}^{N_r \times N_t}$ is assumed. The channel remains constant for each transmission time-slot and changes independently from one slot to another. We assume for simplicity that the channel is perfectly known at both the transmitter and the receiver.

The signal model for the system under consideration is given as

$$\mathbf{y} = \mathbf{H}\mathbf{F}\mathbf{s} + \mathbf{n}, \quad (11)$$

where $\mathbf{y} \in \mathbb{C}^{N_r \times 1}$ is the received signal vector and $\mathbf{n} \in \mathbb{C}^{N_r \times 1}$ denotes the additive noise vector whose elements are drawn independently from a zero-mean circularly symmetric complex Gaussian (ZMCSCG) distribution with variance σ_n^2 . The transmitted signal vector $\mathbf{s} \in \mathbb{C}^{N_t \times 1}$ is precoded using the matrix $\mathbf{F} \in \mathbb{C}^{N_t \times N_t}$ that in general depends on the instantaneous channel

realization \mathbf{H} . Transmitter employs Gaussian signaling² so that $\mathbf{s} \in \mathbb{C}^{N_t \times 1}$ is a ZMCSCG random vector with covariance $\mathbb{E}[\mathbf{s}\mathbf{s}^H] = \mathbf{I}_{N_t}$. It should be noted that even though the vector \mathbf{s} has nominally N_t degrees-of-freedom, the maximum number of streams after precoding will always be K , where K denotes the rank of the channel matrix \mathbf{H} .

In the following, we describe two specific precoder designs applicable to spatial domain SWIPT, the first based on SVD and the second based on GTD.

1) *SVD Based SWIPT*: Recall that the SVD of the channel \mathbf{H} is given by $\mathbf{H} = \mathbf{U}\mathbf{\Sigma}\mathbf{V}^H$, where $\mathbf{\Sigma} \in \mathbb{C}^{N_r \times N_r}$ is a rectangular diagonal matrix whose diagonal elements σ represent the singular values of \mathbf{H} and both $\mathbf{U} \in \mathbb{C}^{N_r \times N_r}$ and $\mathbf{V} \in \mathbb{C}^{N_t \times N_t}$ are unitary matrices. For simplicity, we assume that the positive singular values of the channel are ordered in descending order, that is, $\sigma_1 > \sigma_2 > \dots > \sigma_K > 0$.

The precoder in (11) for the SVD based SWIPT can be written as

$$\mathbf{F} = \mathbf{V}\mathbf{P}^{1/2}, \quad (12)$$

where \mathbf{P} is a square diagonal matrix that has transmit-side power allocation $(p_1, p_2, \dots, p_{N_t})$ on the diagonal. Using linear filter \mathbf{U}^H at the receiver and omitting subchannels that carry only noise parallelizes the MIMO channel into K parallel Gaussian channels with signal-to-noise ratios (SNRs) $p_1\sigma_1^2/\sigma_n^2, \dots, p_K\sigma_K^2/\sigma_n^2$, so that the achievable rate and the harvested energy of the SVD based SWIPT are given by

$$C = \sum_{i \in \mathcal{I}_{SVD}} \log_2 \left(1 + \frac{p_i \sigma_i^2}{\sigma_n^2} \right), \quad (13a)$$

$$EH = \sum_{e \in \mathcal{E}} \eta p_e \sigma_e^2, \quad (13b)$$

respectively. The index sets $\mathcal{E} \subseteq \{1, 2, \dots, K\}$ and $\mathcal{I}_{SVD} \subseteq \{1, 2, \dots, K\} \setminus \mathcal{E}$ represent the subchannels assigned for energy harvesting and information exchange, respectively, and $\eta \in [0, 1]$ is the EH efficiency that is assumed to be independent of the rectifier input signal. Extension to the more realistic EH model where the EH efficiency η is a function of the rectifier input power [30] is presented in Section IV. Under the linear EH model, the information rate or the

²As shown in [35]–[41], ZMCSCG signaling is optimal for SWIPT when the linear EH model is assumed, but suboptimal when the non-linear diode-based EH model is considered. In this paper, the linear EH model or the parametric non-linear EH model from [30] is considered for fixed waveform and an extension to more accurate diode-based EH model and waveform optimization is left as future work.

harvested energy of a specific subchannel for SVD based SWIPT is determined only by the corresponding singular value of the channel and the amount of power allocated to it. While the SVD based structure is optimal for information transmission when combined with power allocation through the water filling algorithm, it is suboptimal when both energy and information need to be transmitted simultaneously in the spatial domain, as shown later in this paper.

2) *GTD Based SWIPT*: We start by recalling the SVD of the channel $\mathbf{H} = \mathbf{U}\mathbf{\Sigma}\mathbf{V}^H$ and multiplying the precoder given in (12) by an orthogonal matrix $\mathbf{X} \in \mathbb{R}^{N_t \times N_t}$ that is designed based on the decomposition $[\mathbf{Q}, \mathbf{R}, \mathbf{X}] \leftarrow \text{GTD}(\mathbf{\Sigma}\mathbf{P}^{1/2}, \mathbf{r})$. As discussed in Section II-A, the positive vector \mathbf{r} needs to satisfy the majorization condition $\mathbf{r} \leq \boldsymbol{\lambda}$, where $\boldsymbol{\lambda}$ contains the non-zero diagonal elements of $\mathbf{\Sigma}(\mathbf{P}^*)^{1/2}$ in descending order. Substituting the modified precoder

$$\mathbf{F} = \mathbf{V}\mathbf{P}^{1/2}\mathbf{X}, \quad (14)$$

with identities $\mathbf{H} = \mathbf{U}\mathbf{\Sigma}\mathbf{V}^H$ and $\mathbf{Q}\mathbf{R}\mathbf{X}^T = \mathbf{\Sigma}\mathbf{P}^{1/2}$ into the signal model (11) and simplifying gives

$$\mathbf{y} = \mathbf{H}\mathbf{F}\mathbf{s} + \mathbf{n} = \mathbf{U}\mathbf{Q}\mathbf{R}\mathbf{s} + \mathbf{n}. \quad (15)$$

Applying linear filter $\mathbf{W}^H = \mathbf{Q}^T\mathbf{U}^H$ on the received vector \mathbf{y} , leads to an end-to-end signal model for the GTD based SWIPT as

$$\tilde{\mathbf{y}} = \mathbf{W}^H\mathbf{y} = \mathbf{R}\mathbf{s} + \tilde{\mathbf{n}}, \quad (16)$$

where $\tilde{\mathbf{n}} = \mathbf{Q}^T\mathbf{U}^H\mathbf{n}$ has the same distribution as \mathbf{n} in (11). According to (10b), the equivalent channel \mathbf{R} after precoding and receive-side filtering is related to the singular values $\mathbf{\Sigma}$ of the fading channel \mathbf{H} through rotations by orthogonal matrices. Since the matrix \mathbf{R} is not in general diagonal, the received signal at a specific subchannel may now contain interference. While this interference is useful for increasing the amount of energy that can be harvested at the receiver, it degrades total information rate if such subchannel is assigned for information exchange and per-stream decoding without interference cancellation is used at the receiver. For the rest of the paper we therefore focus on GTD based designs that create interference-free subchannels for information exchange; *i.e.*, the subchannels used for information decoding at the receive-side correspond to the rows of \mathbf{R} that have only diagonal elements. This allows for per-stream decoding, similar to the case of SVD-based SWIPT, to be used at the receiver.

The achievable rate and the harvested energy for the GTD based SWIPT system described

above are given by

$$C = \sum_{i \in \mathcal{I}_{GTD}} \log_2 \left(1 + \frac{R_{ii}^2}{\sigma_n^2} \right), \quad (17a)$$

$$EH = \sum_{j \in \mathcal{J}} \sum_{l=j}^K \eta R_{jl}^2, \quad (17b)$$

respectively, where R_{ij} denotes the (i, j) th elements of \mathbf{R} and \mathcal{I} and \mathcal{J} are disjoint sets, related to the subchannels that are used for information exchange and energy harvesting at the receive-side, respectively. Note that the effect of power allocation matrix \mathbf{P} is embedded in \mathbf{R} due to the decomposition of $\Sigma \mathbf{P}^{1/2}$.

It is worth noting that the practical implementation issues of the SVD based SWIPT were discussed in [23]. The main practical limitation of the SVD based SWIPT is implementing the required signal processing; *i.e.*, the channel matrix decomposition in the RF band. To overcome this issue, the authors of [23], [25] suggested using analog beamforming based on passive electronic devices to perform channel diagonalization in the RF band as proposed in [47], [48]. Due to the similarities in the SVD and GTD based SWIPT, analog beamforming could potentially be used for the GTD based SWIPT as well. In general, a practical implementation of the proposed approach would require efficient implementation of phase shifting, switching/multiplexing as well as implementing a complex switch-bar matrix operation in hardware including efficient control. However, the work in this paper, similarly to [23], focuses only on the theoretical aspects of the problem and practical implementation of RF hardware is left as future work.

The next subsection demonstrates that GTD based SWIPT can achieve a higher information rate than SVD based SWIPT for a simplified system setup. More particular cases will be considered in Section III after this simple, but illustrative example.

C. Example: SVD and GTD based SWIPT Without Instantaneous Power Constraint

In this subsection we provide a simplified example that highlights the main differences between the SVD and GTD based systems. We also show that the latter provides superior performance in most scenarios and present preliminary results that will be used in the latter parts of the paper. For simplicity, no instantaneous power constraint is enforced; *i.e.*, $\text{tr}(\mathbf{P}) \leq P_t = +\infty$ here.

1) *SVD Based SWIPT*: Consider the problem of minimizing the total transmit power $\text{tr}(\mathbf{P})$ with information rate constraint C_{SVD} and energy harvesting constraint EH_{SVD} in the SVD

based system introduced in Section II-B1. The information rate and harvested energy for a given channel realization and subchannel assignment $\mathcal{E} \subseteq \{1, 2, \dots, K\}$ and $\mathcal{I}_{SVD} \subseteq \{1, 2, \dots, K\} \setminus \mathcal{E}$ are given as in (13). The goal is to find the subchannel assignment (sets \mathcal{E} and \mathcal{I}_{SVD}) and power allocation \mathbf{P} , that jointly satisfy the constraints and minimize the total transmitted power. The power allocation problem for the SVD based SWIPT reads then

$$\underset{\mathbf{P}, \mathcal{I}_{SVD}, \mathcal{E}}{\text{minimize}} \quad \text{tr}(\mathbf{F}\mathbf{F}^H), \quad (18a)$$

$$\text{s.t.} \quad \sum_{i \in \mathcal{I}_{SVD}} \log_2 \left(1 + \frac{p_i \sigma_i^2}{\sigma_n^2} \right) \geq C_{SVD}, \quad (18b)$$

$$\sum_{e \in \mathcal{E}} \eta p_e \sigma_e^2 \geq E H_{SVD}, \quad (18c)$$

where \mathbf{F} is given by (12), $\mathcal{I}_{SVD} \subseteq \{1, \dots, K\} \setminus \mathcal{E}$ are the subchannels assigned for information exchange and $\mathcal{E} \subseteq \{1, \dots, K\}$ denotes to the subchannels that are assigned for energy harvesting. As shown in [23], [24], when there is no instantaneous power constraint, it is optimal to choose only one subchannel for energy harvesting, that is, $\mathcal{E} = \{e\}$ for SVD based SWIPT. The optimal value of e can be found numerically by solving (18) for all K possible subchannel assignments; *i.e.*, $e = 1, 2, \dots, K$, and choosing the one that satisfies the energy harvesting and rate constraints with the least transmitted power. For each subchannel assignment, power is first allocated to satisfy the energy harvesting constraint. Then a water filling type algorithm developed in [26] is used for the information bearing subchannels to obtain power allocation that meets the rate constraint with minimum total transmit power, namely,

$$p_i = \begin{cases} p_w + \sigma_n^2 \left(\frac{1}{\sigma_w^2} - \frac{1}{\sigma_i^2} \right), & i \leq w \quad \text{and} \quad i \neq e \\ 0, & w < i \leq K \quad \text{and} \quad i \neq e \end{cases} \quad (19)$$

where the subchannel index w is given by

$$w = \max \left\{ k \mid 2^{C_{svd}} > \prod_{i=1}^k \frac{\sigma_i^2}{\sigma_k^2} \wedge k \in \{1, 2, \dots, K\} \setminus \{e\} \right\}, \quad (20)$$

and p_w is defined as

$$p_w = \sigma_n^2 \left(\frac{2^{\frac{C_{svd}}{L-1}}}{\left(\prod_{i=1, i \neq e}^w \sigma_i^2 \right)^{\frac{1}{L-1}}} - \frac{1}{\sigma_w^2} \right), \quad (21)$$

where L is the number of subchannels that have nonzero power. Note that for given subchannel gains $\sigma_1^2 > \dots > \sigma_K^2$ and energy harvesting assignment, the water filling algorithm may allocate power to only some of the strongest subchannels in its use. Therefore, the optimal channel assignment for (18) in general has the first $L \leq K$ subchannels active so that $e^* \in \{1, 2, \dots, L\}$ and $\mathcal{I}_{SVD}^* = \{1, 2, \dots, L\} \setminus \{e^*\}$. The power allocation matrix that jointly minimizes the transmitted power with the optimal subchannel assignment $(e^*, \mathcal{I}_{SVD}^*)$ for SVD based SWIPT is denoted \mathbf{P}^* .

2) *GTD Based SWIPT*: Consider now the design of the GTD based precoder (14) when the power allocation matrix \mathbf{P}^* optimized for the SVD based SWIPT is used also by the GTD based precoder. Clearly this may not be the optimal choice for GTD. However, it turns out that the structure of GTD provides enough flexibility to achieve superior information rate compared to SVD most of the time, even when the power allocation is suboptimal.

According to (17), we need to select two disjoint index sets, denoted for the GTD based system \mathcal{I}_{GTD} and \mathcal{J} , that can be different from the index sets \mathcal{I}_{SVD} and \mathcal{E} used for the SVD based SWIPT. As with SVD, using one subchannel for energy harvesting at the receiver is optimal, so that $\mathcal{J} = \{j\}, j \in \{1, 2, \dots, L\}$, and we can define an optimization problem

$$\underset{\mathbf{r} \leq \boldsymbol{\lambda}, \mathcal{I}_{GTD}, j}{\text{maximize}} \quad C_{GTD} = \sum_{i \in \mathcal{I}_{GTD}} \log_2 \left(1 + \frac{R_{ii}^2}{\sigma_n^2} \right), \quad (22a)$$

$$\text{s.t.} \quad \sum_{l=j}^L \eta R_{jl}^2 \geq EH_{GTD}, \quad (22b)$$

where $\mathcal{I}_{GTD} = \{1, \dots, L\} \setminus \{j\}$ is the set of subchannels the used for information decoding at the receive-side. Matrix \mathbf{R} is designed to guarantee interference-free information channels and satisfy the majorization condition $\mathbf{r} \leq \boldsymbol{\lambda}$, where $\boldsymbol{\lambda} = [\lambda_1, \lambda_2, \dots, \lambda_L]^T$ contains the non-zero diagonal elements of $\boldsymbol{\Sigma}(\mathbf{P}^*)^{1/2}$ in descending order, as explained in Section II-B2.

The following theorem shows that with appropriate selection of \mathcal{I}_{GTD} and \mathcal{J} , the solution to the optimization problem (22) provides a GTD based design that achieves an information rate that is better, or at least as good as, than that obtained with SVD, even when the power allocation is specifically designed to optimize the SVD based system.

Theorem 2. Consider the SVD based precoder given in (12). Let $e^* \in \{1, \dots, L\}$ with $L \leq K$ be the optimal subchannel index for energy harvesting and \mathbf{P}^* the optimal power allocation that solve the SVD based design problem (18) for the given rate and energy constraints C_{SVD} and EH_{SVD} , respectively. Given the power allocation \mathbf{P}^* , if $e^* \in \{1, L\}$, the optimal GTD precoder

(14) reduces to the SVD based precoder and both systems have the same performance. When $e^* \notin \{1, L\}$, selecting the non-zero diagonal elements $\mathbf{r} = [r_1, \dots, r_L]^T$ of \mathbf{R} as

$$r_1 = \lambda_2; r_2 = \lambda_3; \dots; r_{L-2} = \lambda_{L-1}; r_{L-1} = \frac{\lambda_1 \lambda_L}{\sqrt{\lambda_1^2 + \lambda_L^2 - \frac{EH_{SVD}}{\eta}}}; r_L = \sqrt{\lambda_1^2 + \lambda_L^2 - \frac{EH_{SVD}}{\eta}}, \quad (23)$$

and choosing $\mathcal{I}_{GTD} = \{1, 2, \dots, L-2, L\}$, $\mathcal{J} = \{L-1\}$, guarantees that the harvested energy satisfies $EH_{GTD} = EH_{SVD}$ and the information rate $C_{GTD} > C_{SVD}$ of the GTD based system is maximized.

Proof: See Appendix A. ■

Theorem 2 can be divided into two cases: 1) When the information rates are equal ($C_{GTD} = C_{SVD}$); and 2) when GTD achieves a higher rate than SVD ($C_{GTD} > C_{SVD}$). The first case occurs when the transmit power for the SVD based precoder is minimized by associating the strongest or the weakest eigenmode of $\Sigma(\mathbf{P}^*)^{1/2}$; *i.e.*, λ_1 or λ_L , with energy harvesting. This corresponds to a scenario where either the energy harvesting or the information rate requirement dominates the constraints, respectively, and no additional benefit can be achieved by the GTD based system.

The case $C_{GTD} > C_{SVD}$ occurs when the energy harvesting constraint (18c) for SVD is satisfied through any subchannel but the best or the worst; *i.e.*, $\mathcal{E} = \{e\}$, $e \notin \{1, L\}$. In this case, \mathbf{R} is obtained via the GTD according to Theorem 1, $[\mathbf{Q}, \mathbf{R}, \mathbf{X}] \leftarrow \text{GTD}(\Sigma(\mathbf{P}^*)^{1/2}, \mathbf{r})$, where \mathbf{r} is given in (23). The only non-zero off-diagonal element of \mathbf{R} is at the $(L-1)$ -th row and reads

$$R_{L-1L} = \frac{1}{r_{L-1}} \sqrt{(\lambda_1^2 - r_{L-1}^2)(r_{L-1}^2 - \lambda_L^2)}, \quad (24)$$

which is non-zero when $e \notin \{1, L\}$. By recalling that $\lambda_k = p_k \sigma_k$, $k = 1, 2, \dots, L$, it is straightforward to verify that matrix \mathbf{R} constructed as in (23) and (24) satisfies $EH_{SVD} = EH_{GTD}$ and $r_{L-1} < \lambda_e$. Together with Remark 1 this implies that more energy is received in the information bearing subchannels of the GTD based system and higher rate can be achieved, see Appendix A for details.

The key difference between the SVD based design and the GTD based system described above is that in the GTD based system the transmitter has the ability to use the subchannel associated with the highest singular value to transmit both information and energy signals while the receiver is able to separate that particular transmission into two different streams; one is used for information and the other is used for energy harvesting. This is in contrast with SVD based

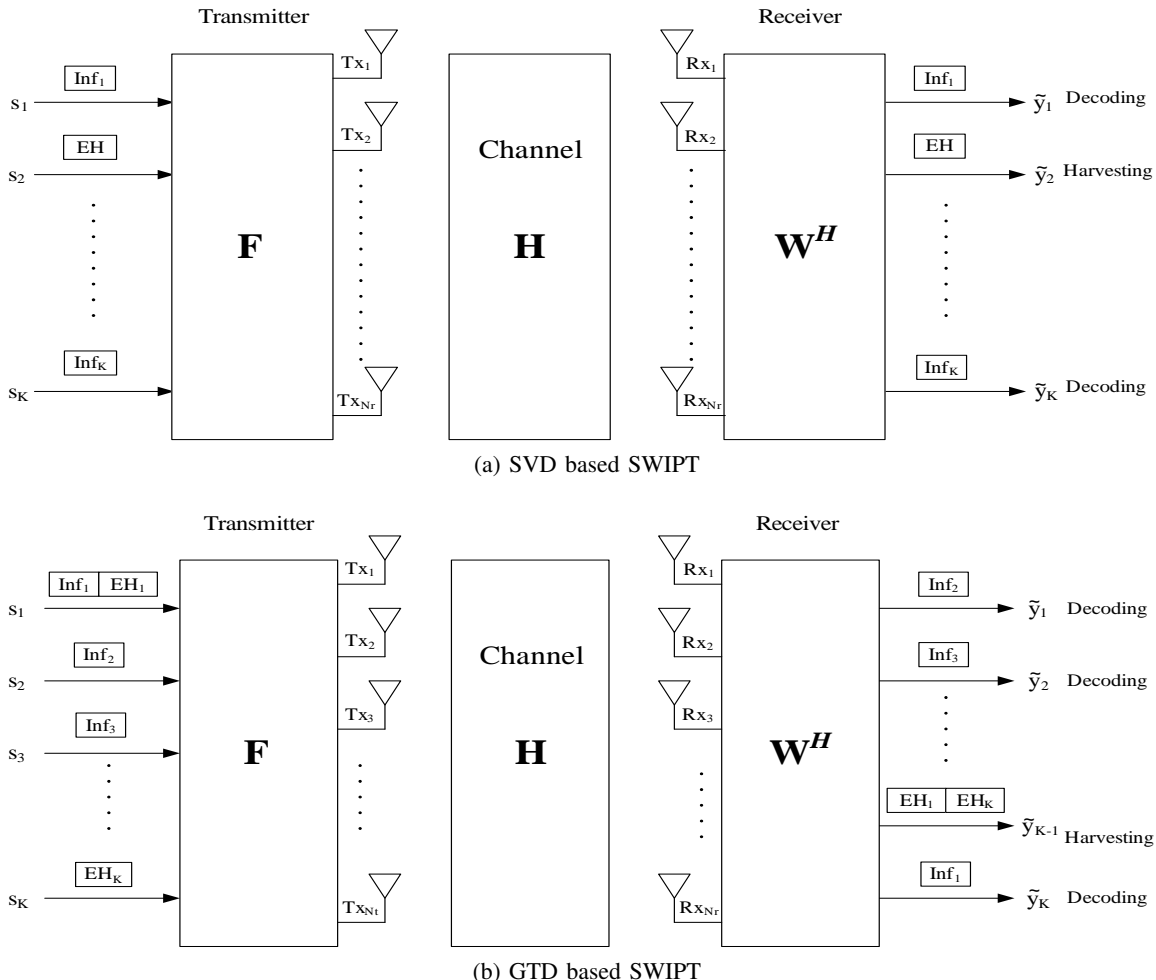


Fig. 1. Comparison between SVD and GTD based SWIPT.

system where each subchannel can carry either information or energy signals [22], [23]. As a result, more transmit power can be used in information bearing subchannels since subchannel with highest singular value is used to transfer information and energy as well. The difference between the GTD approach and the SVD approach is illustrated in Fig. 1.

III. TRANSCIVER DESIGN FOR SWIPT BASED ON GTD

Having demonstrated in Section II-C that the GTD based precoder can outperform the SVD based precoder in a simplified setting, we now consider a more practical problem of minimizing the transmit power given information rate and energy harvesting constraints. Total instantaneous transmit power constraint $\text{tr}(\mathbf{P}) \leq P_t$ is also included. Due to the difference in instantaneous power constraint, the SVD based precoder considered here is slightly different to the case investigated

in [23], [24]. However, due to the space constraints, we omit the details of the SVD based system and concentrate solely on the GTD based SWIPT approach.

A. Transmit Power Minimization for GTD Based SWIPT

As discussed in Section II-B2, the received signal at the k -th subchannel contains interference if the k -th row in \mathbf{R} has off-diagonal elements. Since interference is detrimental for achievable rate, we concentrate here on designing GTD based precoder and receive-side filter that guarantee interference-free subchannels for information transfer. However, as discovered in Section II-C, interference is useful for increasing the amount of energy available for harvesting at the receive-side and, thus, saves transmit power for satisfying the rate constraint.

Based on the above discussion, the following optimization problem can be formulated

$$\underset{\mathbf{P}, \mathbf{r} \leq \lambda, \mathcal{I}, \mathcal{J}}{\text{minimize}} \quad \text{tr}(\mathbf{F}\mathbf{F}^H), \quad (25a)$$

$$\text{s.t.} \quad \sum_{i \in \mathcal{I}} \log_2 \left(1 + \frac{R_{ii}^2}{\sigma_n^2} \right) \geq C, \quad (25b)$$

$$\sum_{j \in \mathcal{J}} \sum_{l=j}^K \eta R_{jl}^2 \geq EH, \quad (25c)$$

$$\sum_{k \in \mathcal{K}} p_k \leq P_t, \quad (25d)$$

where the precoder matrix \mathbf{F} is given by (14), λ represents the positive diagonal elements of $\Sigma \mathbf{P}^{1/2}$ and \mathcal{K} denotes the set of the total available subchannels while $\mathcal{I} \subseteq \mathcal{K}$ and $\mathcal{J} \subseteq \mathcal{K} \setminus \mathcal{I}$ are the sets of subchannels from which the receiver decodes the information and harvests the energy, respectively. In addition to finding power allocation matrix \mathbf{P} , optimal solution requires also to identify which subchannels are used for information and energy transfer, and construction of the precoding and the receive-side matrices \mathbf{F} and \mathbf{W} , respectively.

In the following we show that while the SVD based transceiver design allows a particular subchannel to carry only one type of signal, information or energy, the GTD based system can be designed so that a particular transmitted stream separates at the receiver into two parts; one stream that is used for decoding information and another stream from which energy is harvested, as illustrated in Fig. 1. This is the key difference between the two approaches and is the main reason why the GTD based SWIPT outperforms its SVD counterpart. It should be noted, however,

that the same receive-side stream cannot be used to both harvest energy and decode information in the GTD based system either, rather, the subchannel “re-use” happens at the transmit-side.

To solve (25), we propose a two-stage process that consists of first finding the power allocation matrix \mathbf{P}^* and then using GTD to construct the precoding and the receive-side matrices \mathbf{F} and \mathbf{W} , respectively, as discussed in Section II-B2. The power allocation for information transmission is carried out according to the singular values $\mathbf{\Sigma}$ of the MIMO channel matrix \mathbf{H} using the water filling algorithm that is developed in [26], and then power necessary for satisfying the energy harvesting constraint is added to it. After obtaining the complete power allocation \mathbf{P}^* , GTD is used to decompose the matrix $\mathbf{\Sigma}(\mathbf{P}^*)^{1/2}$ as $[\mathbf{Q}, \mathbf{R}, \mathbf{X}] \leftarrow \text{GTD}(\mathbf{\Sigma}(\mathbf{P}^*)^{1/2}, \mathbf{r})$ to arrive at the input-output relation (16).

To follow the above process, we need to show that the power allocation matrix can be optimized based on the singular values of $\mathbf{\Sigma}$ so that the constraints (25b) and (25c) are both satisfied if the diagonal elements \mathbf{r} of \mathbf{R} in the GTD are chosen appropriately. This design rule relies on the fact that it is optimal to allocate all power that is used for energy harvesting to the strongest singular value σ_1 [23], [24]. Specifically, our goal is to prove that information rate C and harvested energy EH given as

$$C = \sum_{k=1}^{K-1} \log_2 \left(1 + \frac{\phi_k \sigma_k^2}{\sigma_n^2} \right), \quad (26a)$$

$$EH = \eta \cdot (p_{eh} \sigma_1^2 + p_K \sigma_K^2), \quad (26b)$$

can be achieved in GTD based SWIPT. In (26a), the powers $(\phi_1, \phi_2, \dots, \phi_{K-1})$ are obtained by applying the water filling algorithm that is proposed in [26] on the parallel Gaussian channels that have gains $\sigma_1^2, \sigma_2^2, \dots, \sigma_{K-1}^2$ as follows

$$\phi_k = \begin{cases} \phi_w + \sigma_n^2 \left(\frac{1}{\sigma_w^2} - \frac{1}{\sigma_k^2} \right), & k \leq w \\ 0, & w < k \leq K-1 \end{cases} \quad (27)$$

where the subchannel index w is given by

$$w = \max \left\{ j \mid 2^C > \prod_{k=1}^j \frac{\sigma_k^2}{\sigma_j^2} \wedge j \in \{1, 2, \dots, K-1\} \right\}, \quad (28)$$

and ϕ_w is defined as

$$\phi_w = \sigma_n^2 \left(\frac{2 \frac{c}{w}}{\left(\prod_{k=1}^w \sigma_k^2 \right)^{\frac{1}{w}}} - \frac{1}{\sigma_w^2} \right). \quad (29)$$

Note that a similar strategy was used for the SVD based system in Section II-C, but now σ_1 is associated with both information and energy, which is not allowed in the SVD based SWIPT.

For notational simplicity, we consider first the case when the water filling algorithm returns $(\phi_1, \phi_2, \dots, \phi_{K-1})$ that are all non-zero; *i.e.*, $w = K - 1$. The power $p_K > 0$ is set to be as small as possible while keeping the corresponding subchannel active; therefore, the total number of subchannels that have nonzero power is $L = K$. Given that $p_K \sigma_K^2 \ll 1$ and from (26b) we see that p_{eh} is mainly responsible for satisfying the energy harvesting constraint. The reason for the special treatment of p_K will be explained later. From (26), the power allocation matrix that uses the least power and satisfies both constraints is given by

$$\mathbf{P}^* = \text{diag}([\phi_1 + p_{eh}, \phi_2, \dots, \phi_{K-1}, p_K]), \quad (30)$$

where $\mathbf{P} = \text{diag}(\mathbf{p})$ constructs a square diagonal matrix with \mathbf{p} on the diagonal. Therefore, problem (25) is feasible if

$$\sum_{k=1}^{K-1} \phi_k + p_{eh} + p_K \leq P_t, \quad (31)$$

holds and (26a)–(26b) match (25b)–(25c) exactly.

If the power allocation is carried out as in (26a) and (26b), the GTD of $\mathbf{\Sigma}(\mathbf{P}^*)^{1/2}$ has to be done using \mathbf{r} that results in \mathbf{R} that satisfies the information rate and energy harvesting constraints given in (25b) and (25c). As discussed in Section II-C, the chosen \mathbf{r} must be multiplicatively majorized by the positive diagonal elements of $\mathbf{\Sigma}(\mathbf{P}^*)^{1/2}$, that is, $\mathbf{r} \leq \lambda$. Using \mathbf{r} given in Theorem 2 satisfies this condition and results in a receive-side subchannel assignment where $\mathcal{J} = \{K - 1\}$ is used for energy harvesting and $\mathcal{I} = \{1, \dots, K - 2, K\}$ for information decoding. To show that this GTD structure indeed solves (25), we need to verify that the resulting \mathbf{R} with \mathcal{I} and \mathcal{J} as above satisfy (25b) and (25b). For energy harvesting, we note that R_{K-1K-1} coincides with r_{L-1} given in (23) and R_{K-1K} is equal to (24) if we set $L = K$. From (23), to have a non-zero $(K - 1)$ -th receive-side subchannel for energy harvesting, we need $\lambda_K = p_K \sigma_K > 0 \iff p_K > 0$. This is the reason why $p_K > 0$ even though it does not contribute to satisfying the constraints. With the above, substituting $\lambda_1 = \sqrt{p_{eh} + \phi_1} \sigma_1$ and $\lambda_K = \sqrt{p_K} \sigma_K$ to (23) and (24) verifies that

$R_{K-1K-1}^2 + R_{K-1K}^2 = p_{eh}\sigma_1^2 + p_K\sigma_K^2$, so that (25c) and (26b) are equal, as desired.

To guarantee that the information rates in (25b) and (26a) are equal, we need to have

$$\sum_{k=1}^{K-1} \log_2 \left(1 + \frac{\phi_k \sigma_k^2}{\sigma_n^2} \right) = \sum_{i \in \mathcal{I}} \log_2 \left(1 + \frac{r_i^2}{\sigma_n^2} \right), \quad (32)$$

where $R_{ii} = r_i$. As discussed in Section II-A, vector \mathbf{r} given in (23) leads to subchannels in \mathcal{I} that contain no interference, that is, the corresponding rows of \mathbf{R} have only diagonal elements. From (23) we recall that $r_1 = \lambda_2 = \sqrt{\phi_2}\sigma_2; \dots; r_{K-2} = \lambda_{K-1} = \sqrt{\phi_{K-1}}\sigma_{K-1}$ so that the corresponding $K - 2$ subchannels related to information transfer in (25b) and (26a) are just permutations of each other. To guarantee equal information rate in both cases, the subchannel associated with r_K must therefore satisfy $\log_2(1 + \phi_1\sigma_1^2/\sigma_n^2) = \log_2(1 + r_K^2/\sigma_n^2)$. Substituting r_K given in (23) on the RHS yields the equality leads to

$$\log_2 \left(1 + \frac{r_K^2}{\sigma_n^2} \right) = \log_2 \left(1 + \frac{\lambda_1^2 + \lambda_K^2 - \frac{EH}{\eta}}{\sigma_n^2} \right) \quad (33a)$$

$$= \log_2 \left(1 + \frac{(p_{eh} + \phi_1)\sigma_1^2 + p_K\sigma_K^2 - (p_{eh}\sigma_1^2 + p_K\sigma_K^2)}{\sigma_n^2} \right) \quad (33b)$$

$$= \log_2 \left(1 + \frac{\phi_1\sigma_1^2}{\sigma_n^2} \right), \quad (33c)$$

where the second equality follows from the fact that $\lambda_1 = \sqrt{p_{eh} + \phi_1}\sigma_1$, $\lambda_K = \sqrt{p_K}\sigma_K$ and $EH/\eta = p_{eh}\sigma_1^2 + p_K\sigma_K^2$. Thus, vector \mathbf{r} given in (23) guarantees that (26a)–(26b) match (25b)–(25c) and power allocation (30) satisfies the constraints with minimum total transmit power if (25) is feasible.

Finally, if the water filling algorithm allocates power to only the first w strongest subchannels ($w < K - 1$) so that $\phi_{w+1} = \phi_{w+2} = \dots = \phi_{K-1} = 0$, the above development still holds when σ_K is replaced with σ_{w+1} and p_K by p_{w+1} everywhere; thus, the number of the subchannels with nonzero powers $L = w + 1$. For simplicity, Algorithm 1 summarizes the solution to the problem (25) for the case $L = K - 1$.

B. Complexity Analysis

In this subsection, we briefly summarize the complexity of the GTD and SVD based SWIPT schemes. Following [43], [44], the complexity of the main steps in GTD based SWIPT can be obtained as given in Table I. Note that the complexity in Step 2 is due to the water filling

Algorithm 1 Solution to the problem (25)

- 1: $[\mathbf{U}, \mathbf{\Sigma}, \mathbf{V}] \leftarrow \text{SVD}(\mathbf{H})$
 - 2: Obtain $[\phi_1, \phi_2, \dots, \phi_{K-1}]$ that satisfy (25b) using (27), (28) and (29), given channel gains $\sigma_1^2, \sigma_2^2, \dots, \sigma_{K-1}^2$.
 - 3: Set minimum transmit power $p_K > 0$, so that the K -th transmit stream is active
 - 4: Set $p_{eh} = (EH - p_K \sigma_K^2) / \eta \sigma_1^2$
 - 5: **if** (31) holds **then**
 - 6: Set power allocation \mathbf{P}^* as in (30)
 - 7: Set vector \mathbf{r} as in (23)
 - 8: $[\mathbf{Q}, \mathbf{R}, \mathbf{X}] \leftarrow \text{GTD}(\mathbf{\Sigma}(\mathbf{P}^*)^{1/2}, \mathbf{r})$
 - 9: Transmit using precoder (14) and apply filter (16) at the receiver
 - 10: Harvest energy from the subchannel $\mathcal{J} = \{K-1\}$
 - 11: Decode information from the subchannels $\mathcal{I} = \{1, \dots, K\} \setminus \mathcal{J}$
 - 12: **else**
 - 13: Problem (25) is infeasible for GTD based SWIPT
 - 14: **End if**
-

algorithm that has complexity of $O(K^2)$ and that both schemes require the calculation of an SVD and matrix \mathbf{F} . The additional complexity of GTD based SWIPT is $O(K^2)$ and due to Steps 3 and 4 that are not required in the SVD based SWIPT. On the other hand, because the SVD based SWIPT examines K of the subchannels assignment, Step 2 is executed K -times in order to obtain the minimum required power allocation. This implies that Step 2 for SVD based SWIPT requires in fact $O(K^3)$ computations to obtain the solution. The leading term in complexity of both schemes is, however, due to the calculation of the SVD in Step 1 and, thus, both schemes are $O(N_t N_r K)$.

TABLE I
COMPLEXITY OF THE GTD BASED SWIPT

Step	Operation	Complexity
1	Compute SVD $\mathbf{H} = \mathbf{U}\mathbf{\Sigma}\mathbf{V}^H$	$O(N_t N_r K)$
2	Calculate the power allocation using (30)	$O(K^2)$
3	Calculate $\mathbf{\Sigma}(\mathbf{P}^*)^{1/2}$	$O(K)$
4	Apply GTD on $\mathbf{\Sigma}(\mathbf{P}^*)^{1/2}$	$O(K^2)$
5	Obtain \mathbf{F} as in (14)	$O(N_t K)$

IV. NON-LINEAR ENERGY HARVESTING MODEL

In this section, we extend the developed GTD design for the non-linear EH model proposed in [30]. Assuming that each EH subchannel is assigned one rectifier, the energy harvested at the

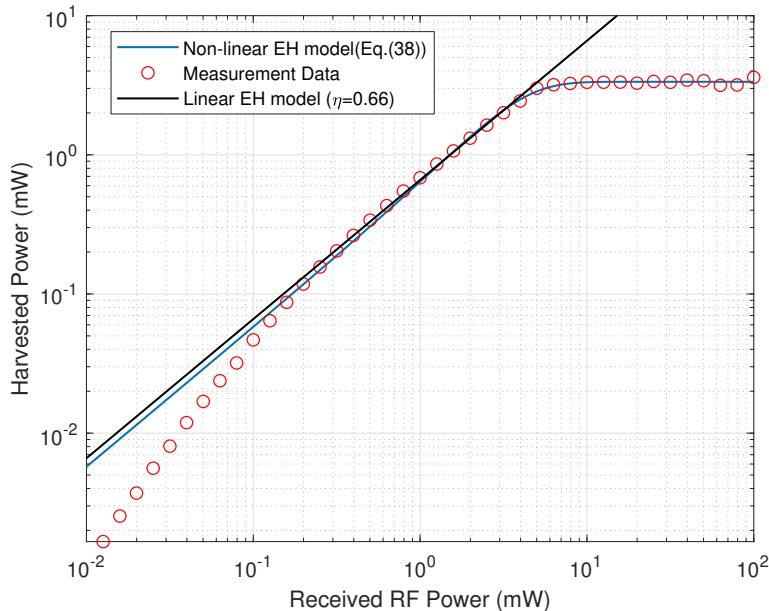


Fig. 2. Comparison between the non-linear EH model, the linear EH model, and measurement data from a practical 5-stage rectifier circuit in [49, Fig.3]. The parameters $M_j = 3.348$, $a_j = 0.6152$ and $b = 1.55$ in (34) were obtained by a standard curve fitting tool when the rectifier input power p_j^{RF} is in mWs.

j -th subchannel for the GTD based system can be written as

$$EH_j = M_j \cdot \frac{1 - e^{-a_j p_j^{RF}}}{1 + e^{-a_j p_j^{RF} + a_j b_j}}, \quad (34)$$

where $p_j^{RF} = \sum_{l=j}^K R_{jl}^2$ is the received RF power at the j -th subchannel and $\{a_j, b_j, M_j\}$ are tunable parameters that characterize the EH behavior of the rectifier at the j -th subchannel (for more details, see [30], [31], [41]). In practice, these parameters are found by curve fitting on measurements as demonstrated in Fig. 2. Note that now the EH efficiency $\eta_j(p_j^{RF}) = EH_j/p_j^{RF}$ is not a constant but a non-linear function of the rectifier input power p_j^{RF} . However, for a limited range of received / harvested power, the linear model can be used as an approximation of the non-linear EH model; for example in the case of Fig. 2 when the harvested energy is roughly between 0.1 mW and 2 mW. Within this region, the rectifier operates efficiently and the non-linear model (34) yields a good approximation to the practical implementation.

Within the “linear region” of the rectifier, the development in Section III that assumed simplified linear EH model is still valid; *i.e.*, all power that is used for energy harvesting should be allocated to the subchannel corresponding to the highest singular value σ_1 . Recalling that $p_j^{RF} \approx p_{eh} \sigma_1^2$ since the contribution from the K th subchannel is negligible, the power allocation

at the transmitter that guarantees harvested energy equal to EH is now given by

$$p_{eh} = \frac{1}{a\sigma_1^2} \ln \left(\frac{M + e^{ab}EH}{M - EH} \right), \quad (35)$$

where we have dropped the subscripts j since the subchannel allocation is fixed as detailed in Section III. As before, the transmitter allocates power to the information streams according to (27)–(29). To construct the transmit- and receive-side matrices \mathbf{F} and \mathbf{W} , respectively, the vector \mathbf{r} used in the GTD algorithm is obtained from (23). The only change is that the constant η is now replaced by $\eta(p^{RF})$ that can be calculated after power allocation (35) is carried out.

Finally, let us consider the case when one subchannel is used for energy harvesting as before, but the EH requirement is above the efficient region of the rectifier. As shown in Fig. 2, in this region an increase in the received RF power increases the harvested energy only marginally since the rectifier is close to saturation or has already saturated. To solve this issue while keeping the structure derived in Section III, one could split the received RF power over multiple rectifiers as proposed in [34], [50]. Using the multiple rectifiers solution provided in [34] with the proposed GTD approach requires solving a joint optimization problem of finding the power allocation p_{eh} along with the split ratios that distribute the received RF power over multiple rectifiers. In this case, the developed GTD structure in this paper is still applicable if sufficient number of rectifiers are available so that they all operate in the efficient region. We conjecture that this structure is in fact optimal for the proposed system with EH model [30], but this line of research is left as future work. Another option would be to use multiple subchannels, each with one rectifier, for energy harvesting. This requires developing new subchannel assignment and power allocation algorithms for the system and is not considered in this paper. It should also be remarked that (34) is not accurate when the received RF power that is required to satisfy the EH requirement is below 0.1 mW [41]. Therefore, more accurate model, such as, the diode-based EH model investigated in [35]–[41] should be used. When the diode-based EH model is used, the energy conversion efficiency ; *i.e.*, η is known to be non-linear function with respect to the received signal \mathbf{y} . Hence, incorporating such model with the GTD based SWIPT requires associating the problem of joint power allocation and subchannel assignment with the distribution of the transmitted signal and its waveform design. However, using the diode model with the developed GTD approach is left as future work.

V. NUMERICAL RESULTS

In this section, simulation results are presented to compare the performance of GTD and SVD based precoding methods for SWIPT. A Rayleigh block fading spatially uncorrelated MIMO channel is considered, so that the entries of \mathbf{H} are independent ZMCSCG random variables with variance $\sigma_h^2 = ad^{-\gamma}$ where $a = 0.1$ is the path loss factor, $d = 15$ m is the transmitter to receiver distance and $\gamma = 3$ represents the path loss exponent. The noise power is set to -60 dBm. A symmetric antenna setup $N_t = N_r = 4$ is assumed in all simulations. The power is measured in watts (W) and the information rate is measured in bits per second per hertz (bps/Hz). Both the linear and the non-linear EH models are considered and the relevant parameters of the EH models are as in Fig. 2. The results are averaged over 10^6 independent channel realizations using Monte Carlo simulations.

In Figures 3 and 4, the blue color refers to the GTD based SWIPT and the red color to the SVD based SWIPT. In all figures the lines denote the results related to the linear EH model used in Sections II and III, while the markers represent the results of the non-linear EH model introduced in Section IV. In all cases, the GTD based precoder is optimized as described in Section III-A. The SVD based precoder is optimized similarly, but the details are omitted due to space constraints. It can be observed that the performance gap between the linear and the non-linear EH models is small in all selected cases since the EH requirement lies within the “linear region” of the EH circuit as discussed in Section IV.

Figure 3 shows plots of outage probability versus the instantaneous total transmit power constraint P_t under different data rate C and energy harvesting EH requirements. The outage is defined as an event when one or both of the constraints cannot be satisfied for the given power constraint P_t . In Fig. 3(a), the outage probability of the GTD based SWIPT decays steeply as a function of the total transmit power. In contrast, the curves representing the SVD based SWIPT decay slowly and exhibit much higher outage probabilities throughout the entire range. It is also clear that for a constant rate constraint $C = 15$ bps/Hz, increasing the energy harvesting requirement from $EH = 0.1$ mW to $EH = 0.5$ mW has significantly less impact on the outage probability of the GTD base system compared to the SVD based one. The dramatic difference between the two techniques can be highlighted by considering a case of moderate power, rate and energy harvesting constraints, namely, $P_t = 4$ W, $C = 15$ bps/Hz and $EH = 0.3$ mW. Under these conditions, the GTD based system shows 4% outage probability, while the SVD

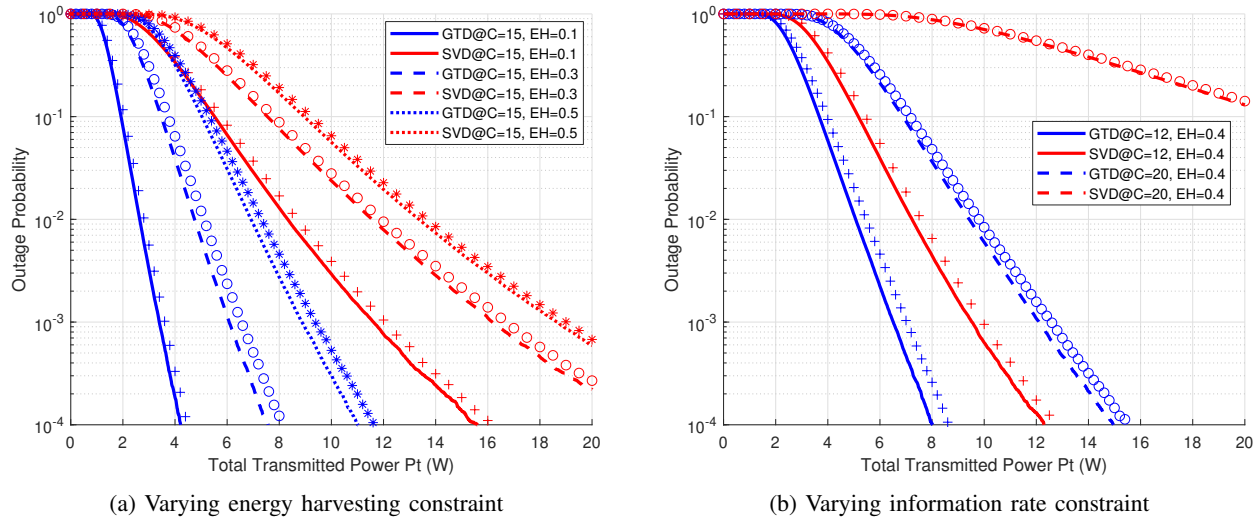


Fig. 3. Outage probability vs. total transmit power constraint P_t for different energy harvesting and rate requirements (C in bps/Hz, EH in mW).

based system has 69% outage probability, making the system unusable. The difference in the performance is explained by the fact that the best eigenchannel in the GTD based precoder can be assigned to carry both information and energy simultaneously, while for the SVD based precoder each eigenchannel can carry either information or energy, but not both at the same time. Similar behavior can be observed in Fig. 3(b), where the GTD based approach provides superior performance in all considered cases. For example, given energy harvesting constraint $EH = 0.4$ mW and 15% outage probability, increasing the rate constraint C from 12 to 20 bps/Hz requires the average transmit power to be increased by 3 W for the GTD based approach while 14 W more power is needed for the SVD based approach.

Having demonstrated that for given instantaneous transmit power constraint P_t , the probability that a GTD based system fails to meet the energy harvesting and information rate targets is orders of magnitude lower than with SVD based system, in Fig. 4 we examine the average transmitted powers of both systems when the instantaneous power constraint is relaxed as $P_t = +\infty$. Note that the SVD based SWIPT in this case becomes similar to those investigated in [24] and [23]. The considered setup guarantees that both SWIPT strategies always succeed in meeting the constraints, while minimizing the total transmit power as explained in Section III.

Figure 4(a) plots the average total transmit power versus rate constraint for both precoding schemes. For a given value of EH , increasing the rate requirement for the GTD based system shows only mild increase in the average transmit power. In contrast, the curves representing

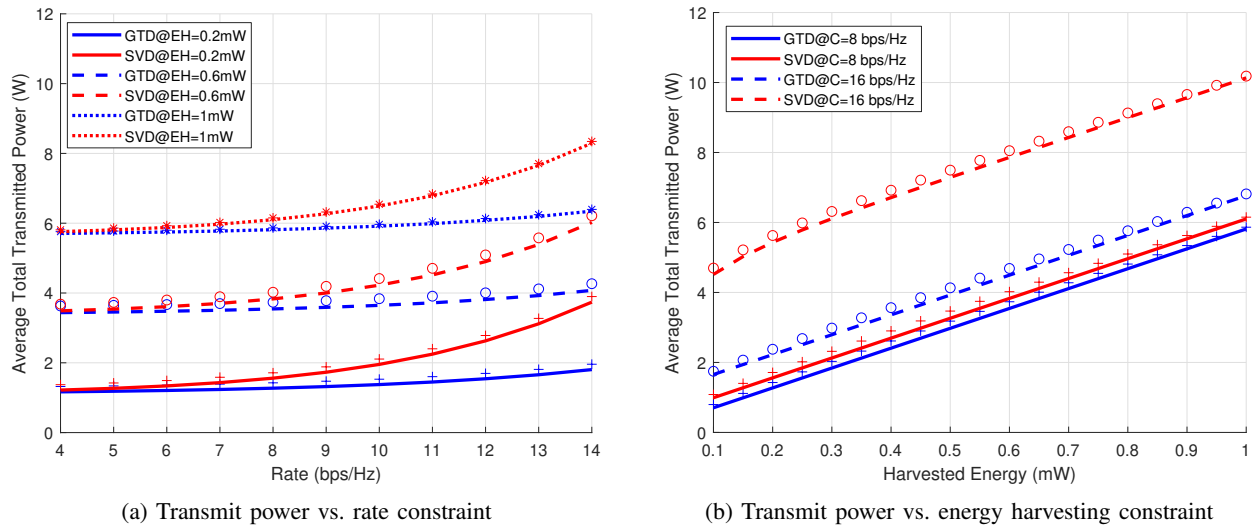


Fig. 4. Average total transmitted power with optimum power allocation and no instantaneous power constraint, $P_t = +\infty$.

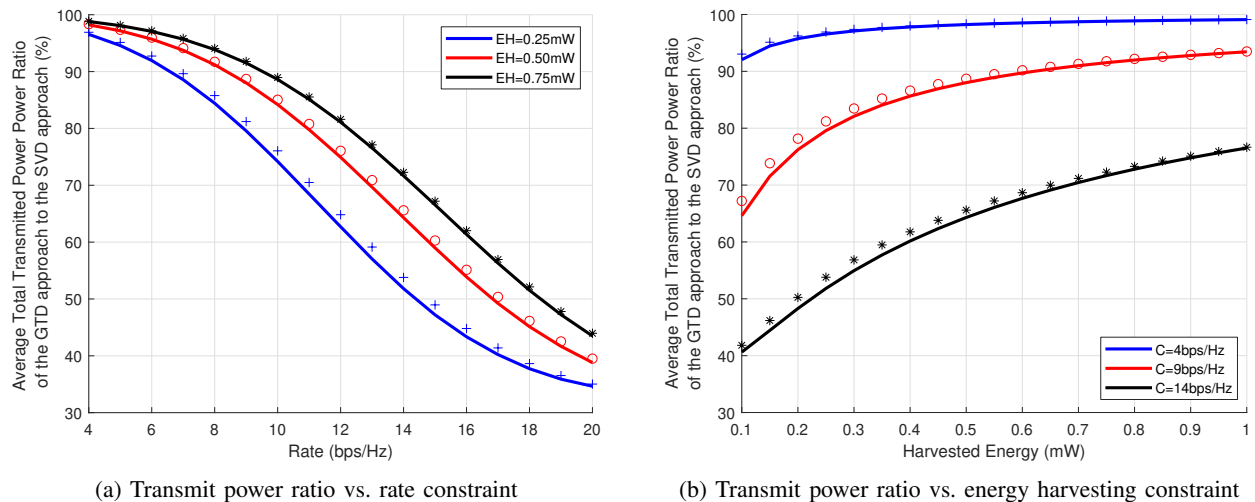


Fig. 5. Average transmit power ratio between GTD and SVD based SWIPT with optimum power allocation and no instantaneous power constraint, $P_t = +\infty$.

the SVD based system rise sharply for the higher values of the rate constraint. For example, increasing the rate constraint C from 9 to 13 bps/Hz while holding EH fixed at 0.6 mW requires increasing the average total transmitted power by 0.3 W and 1.4 W for the GTD and SVD based approaches, respectively. The average total transmit power as a function of energy harvesting constraint is examined in Fig. 4(b). The results clearly show that using GTD based SWIPT leads to significant saving of transmitted power in comparison with the SVD based SWIPT, especially for higher rate constraints. For example, $EH = 0.4$ mW, $C = 16$ bps/Hz can be achieved using average power of 3.6 W with GTD, while approximately 7 W are required with SVD.

To investigate the relative performance of the two SWIPT schemes in more detail, Fig. 5 plots the ratio between the average total transmit power for the GTD and SVD based systems versus the rate and energy harvesting constraints. As in Fig. 4, the scenario of no instantaneous power constraint ($P_t = +\infty$) is considered. The results clearly show that a significant saving in the transmitted power can be achieved for a wide range of system parameter values by using the proposed GTD based approach instead of the conventional SVD based approach.

VI. CONCLUSIONS

In this paper, we have proposed a new approach for SWIPT, based on the GTD, in a point-to-point MIMO communication system. The GTD structure is exploited to create an interfering subchannel to satisfy the energy harvesting requirement while maintaining the best subchannels for information exchange. We have derived the optimal GTD structure that maximizes the information rate for a given power allocation and energy harvesting constraint. We have proposed an algorithm that obtains the optimal subchannel assignment and power allocation to minimize the total transmitted power for given information and energy harvesting constraints. We compare the proposed approach against the state-of-the-art SVD based scheme. Both the theoretical and the numerical simulation results show that the GTD based SWIPT well outperforms the SVD based SWIPT. The improvements provided by the proposed method arise from the fact that the GTD allows the transmitter to use the strongest subchannel to transfer both energy and information jointly which is not possible in the SVD based SWIPT. Extension of the present work to a more realistic energy harvesting model is important future work and would open up new possibilities for optimization of the system, for example via waveform design. Another research avenue worth exploring in future, is the practical implementation aspects of GTD based SWIPT in light of advances in RF CMOS design of switching, phase shifters, and EH circuits.

APPENDIX A

PROOF OF THEOREM 2

Let $\mathcal{J} = \{j\}$ so that the energy harvested at the GTD based receiver is given by

$$EH_{GTD} = \eta(R_{jj}^2 + R_{jj+1}^2 + \cdots + R_{jL}^2). \quad (36)$$

For simplicity, we assume that $\eta = 1$ where the proof is valid for any value of η . Substituting (6) in (9a) and following [42], it can be shown that the value of the diagonal element $R_{jj} = r_j$ is related to the off-diagonal elements on the same row as

$$R_{jj+1}^2 + \cdots + R_{jL}^2 = \frac{1}{R_{jj}^2} (\alpha_j^2 - R_{jj}^2) (R_{jj}^2 - \beta_j^2), \quad (37)$$

where the parameters α_j and β_j are set in the GTD algorithm during the j -th iteration as discussed in Section II-A. From (36) and (37) the harvested energy as a function of the predefined diagonal elements \mathbf{r} is thus given by

$$EH_{GTD} = r_j^2 + \frac{1}{r_j^2} (\alpha_j^2 - r_j^2) (r_j^2 - \beta_j^2), \quad (38)$$

where the values of α_j and β_j also depend on \mathbf{r} . Clearly (38) implies that for the subchannels $i \in \mathcal{I}_{GTD}$ carrying data, we must have $\alpha_i = r_i$ or $\beta_i = r_i$ in the GTD algorithm at the i -th iteration to guarantee interference free information transmission.

The multiplicative majorization condition $\mathbf{r} \leq \boldsymbol{\lambda}$ and ordering $\lambda_1 \geq \lambda_2 \geq \dots \geq \lambda_L$ imply that

$$\lambda_L \leq r_k \leq \lambda_1, \quad \forall k = 1, 2, \dots, L, \quad (39)$$

where $\boldsymbol{\lambda}$ is a vector constructed from the diagonal elements of the matrix $\boldsymbol{\Sigma}(\mathbf{P}^*)^{1/2}$. According to [42], the values of α_k and β_k must satisfy

$$\lambda_L < \alpha_k \leq \lambda_1, \quad (40a)$$

$$\lambda_L \leq \beta_k < \lambda_1, \quad (40b)$$

that together with (39) limit the range of C_{GTD} and EH_{GTD} . This leads to two different cases when $EH_{GTD} = EH_{SVD}$ is guaranteed, namely $C_{GTD} = C_{SVD}$ and $C_{GTD} > C_{SVD}$, depending on how the power and subchannels are allocated in the SVD based system as shown below.

Let us denote $e = e^*$ for the subchannel assigned for energy harvesting by the SVD based precoder so that $\mathcal{E} = \{e\}$ and $\mathcal{I}_{SVD} = \{1, \dots, L\} \setminus \{e\}$ are the optimal subchannel assignments. The energy harvested $EH_{SVD} = \lambda_e^2$ by the SVD based system satisfies $\lambda_L^2 \leq EH_{SVD} \leq \lambda_1^2$. We show below that if $e \notin \{1, L\}$, the subchannels $\mathcal{J} = \{j\}$ and $\mathcal{I}_{GTD} = \{1, \dots, L\} \setminus \{j\}$ and the vector $\mathbf{r} \leq \boldsymbol{\lambda}$ can be designed so that the energy harvested by the GTD based system (38) satisfies $EH_{GTD} = EH_{SVD}$ with $\lambda_L < r_j < \lambda_e$. Since the energy harvesting constraint is satisfied

in part through interference, more power can be allocated to information transmission leading to information rate $C_{GTD} > C_{SVD}$. The special case $e \in \{1, L\}$, on the other hand, leads to $EH_{GTD} = EH_{SVD}$ and $C_{GTD} = C_{SVD}$.

According to (38), the contribution of interference to the harvested energy is highest when α_j is maximized and β_j minimized. For given r_j , the constraints (40) imply that a maximum amount of interference is obtained when $\alpha_j = \lambda_1$ and $\beta_j = \lambda_L$. However, α_j and β_j are not free parameters but set during the j -th iteration of the GTD algorithm and depend in general on the first j entries r_1, r_2, \dots, r_j of \mathbf{r} . Based on the GTD algorithm discussed in Section II-A, $\alpha_j = \lambda_1$ and $\beta_j = \lambda_L$ can be obtained simultaneously if and only if energy is harvested from the subchannel $j = L - 1$ and

$$r_1 = \lambda_2; r_2 = \lambda_3; \dots; r_{L-2} = \lambda_{L-1}, \quad (41)$$

as given in (23). This implies that the GTD based system decodes information always from the subchannels $i = 1, 2, \dots, L - 2, L$ and there is no need for numerical optimization of subchannel assignment as in the SVD based system.

Based on the above, let us now fix the subchannel assignment for GTD as $\mathcal{J} = \{L - 1\}$, $\mathcal{I}_{GTD} = \{1, \dots, L - 2, L\}$ and set r_1, \dots, r_{L-2} as in (41). Substitute $\alpha_{L-1} = \lambda_1$, $\beta_{L-1} = \lambda_L$ and $EH_{GTD} = EH_{SVD} = \lambda_e^2$ into (38), so that after some algebraic manipulations we get r_{L-1} as given in (23). Since the interference term is maximized in (38), the value $r_{L-1} \leq \lambda_e$ is the minimum possible that satisfies the energy harvesting constraint $EH_{GTD} = EH_{SVD}$. The majorization condition, together with (41) provides r_L as also given in (23), and the only non-zero off-diagonal element in \mathbf{R} , R_{L-1L} , is given as (24) and follows from (38). The construction (23) satisfies now $\mathbf{r} \leq \boldsymbol{\lambda}$ and yields a matrix \mathbf{R} for which $EH_{GTD} = EH_{SVD} = \lambda_e^2$ given any power allocation \mathbf{P} and subchannel assignment $\mathcal{E} = \{e\}$, $\mathcal{I}_{SVD} = \{1, \dots, L\} \setminus \{e\}$ in the SVD based system.

Given \mathbf{r} as described above, two cases can be identified depending on how the SVD based system allocates the energy harvesting subchannel, namely, 1) when $e \in \{1, L\}$; and 2) when $e \notin \{1, L\}$. In the first case (24) implies directly $r_{L-1} = \lambda_e$ and the interference term in (38) vanishes. Since \mathbf{r} is now just a permutation of $\boldsymbol{\lambda}$, SVD and GTD based systems are equivalent so that $EH_{SVD} = EH_{GTD}$ and $C_{GTD} = C_{SVD}$. For the second case $r_{L-1} < \alpha_{L-1} = \lambda_1$ and $r_{L-1} > \beta_{L-1} = \lambda_L$ so that the interference term in (38) is positive and $r_{L-1} < \lambda_e$. To show

that this improves the rate of the GTD based system, the condition $\sum_{i \in \mathcal{I}_{GTD}} \log_2(1 + r_i^2 \sigma_n^{-2}) > \sum_{i \in \mathcal{I}_{SVD}} (1 + \lambda_i^2 \sigma_n^{-2})$ must hold. To check this condition is always true for the assignment discussed above, we write the achievable rate of the GTD system in term of λ 's by using (41) and substitute the value of r_L as given in (23) to the above condition to obtain

$$\underbrace{\sum_{i=2}^{L-1} \log_2 \left(1 + \frac{\lambda_i^2}{\sigma_n^2} \right) + \log_2 \left(1 + \frac{\lambda_1^2 + \lambda_L^2 - \lambda_e^2}{\sigma_n^2} \right)}_{C_{GTD}} > \underbrace{\sum_{\substack{i=1 \\ i \neq e}}^L \log_2 \left(1 + \frac{\lambda_i^2}{\sigma_n^2} \right)}_{C_{SVD}}. \quad (42)$$

From (42) the condition for $C_{GTD} > C_{SVD}$ can be directly written as

$$\log_2 \left(1 + \frac{\lambda_e^2}{\sigma_n^2} \right) + \log_2 \left(1 + \frac{\lambda_1^2 + \lambda_L^2 - \lambda_e^2}{\sigma_n^2} \right) > \log_2 \left(1 + \frac{\lambda_1^2}{\sigma_n^2} \right) + \log_2 \left(1 + \frac{\lambda_L^2}{\sigma_n^2} \right) \quad (43a)$$

$$\iff \log_2 \left[\left(1 + \frac{\lambda_1^2 + \lambda_L^2}{\sigma_n^2} \right) + \frac{\lambda_1^2 \lambda_e^2 + \lambda_L^2 \lambda_e^2 - \lambda_e^4}{\sigma_n^4} \right] > \log_2 \left[\left(1 + \frac{\lambda_1^2 + \lambda_L^2}{\sigma_n^2} \right) + \frac{\lambda_1^2 \lambda_L^2}{\sigma_n^4} \right] \quad (43b)$$

$$\iff \lambda_e^2 (\lambda_1^2 + \lambda_L^2 - \lambda_e^2) - \lambda_1^2 \lambda_L^2 > 0. \quad (43c)$$

To prove (43c) indeed holds, define $y > 0$ and $z > 0$ to be real positive numbers. Because $\lambda_L < \lambda_e < \lambda_1$, we can write $\lambda_e^2 = \lambda_L^2 + y$ and $\lambda_1^2 = \lambda_L^2 + y + z$ and substitute into (43c). After some simplifications we get $yz > 0$, and, thus $C_{GTD} > C_{SVD}$, completing the proof of Theorem 2.

ACKNOWLEDGEMENT

The authors are grateful to Prof. Risto Wichman from the School of Electrical Engineering, Aalto University for his helpful suggestions for improving this manuscript.

REFERENCES

- [1] S. Sudevalayam and P. Kulkarni, "Energy harvesting sensor nodes: Survey and implications," *IEEE Communications Surveys & Tutorials*, vol. 13, no. 3, pp. 443–461, 2011.
- [2] P. Lu, X.-S. Yang, J.-L. Li, and B.-Z. Wang, "A compact frequency reconfigurable rectenna for 5.2-and 5.8-GHz wireless power transmission," *IEEE Transactions on Power Electronics*, vol. 30, no. 11, pp. 6006–6010, 2015.
- [3] S. D. Assimonis, S.-N. Daskalakis, and A. Bletsas, "Sensitive and efficient RF harvesting supply for batteryless backscatter sensor networks," *IEEE Transactions on Microwave Theory and Techniques*, vol. 64, no. 4, pp. 1327–1338, 2016.
- [4] Y.-S. Chen and C.-W. Chiu, "Maximum achievable power conversion efficiency obtained through an optimized rectenna structure for RF energy harvesting," *IEEE Transactions on Antennas and Propagation*, vol. 65, no. 5, pp. 2305–2317, 2017.
- [5] C. Song, Y. Huang, J. Zhou, J. Zhang, S. Yuan, and P. Carter, "A high-efficiency broadband rectenna for ambient wireless energy harvesting," *IEEE Transactions on Antennas and Propagation*, vol. 63, no. 8, pp. 3486–3495, 2015.
- [6] I. Krikidis, S. Timotheou, S. Nikolaou, G. Zheng, D. W. K. Ng, and R. Schober, "Simultaneous wireless information and power transfer in modern communication systems," *IEEE Communications Magazine*, vol. 52, no. 11, pp. 104–110, 2014.

- [7] L. R. Varshney, "Transporting information and energy simultaneously," in *Proc. IEEE International Symposium on Information Theory (ISIT)*, July 2008, pp. 1612–1616.
- [8] P. Grover and A. Sahai, "Shannon meets Tesla: Wireless information and power transfer," in *Proc. IEEE International Symposium on Information Theory (ISIT)*, July 2010, pp. 2363–2367.
- [9] R. Zhang and C. K. Ho, "MIMO broadcasting for simultaneous wireless information and power transfer," *IEEE Transactions on Wireless Communications*, vol. 12, no. 5, pp. 1989–2001, 2013.
- [10] F. Benkhelifa, A. S. Salem, and M.-S. Alouini, "Rate maximization in MIMO decode-and-forward communications with an EH relay and possibly imperfect CSI," *IEEE Transactions on Communications*, vol. 64, no. 11, pp. 4534–4549, 2016.
- [11] F. Benkhelifa, A. S. Salem, and M. Alouini, "SWIPT in multiuser MIMO decode-and-forward relay broadcasting channel with energy harvesting relays," in *IEEE Globecom Workshops*, Dec. 2016, pp. 1–7.
- [12] S. Timotheou, I. Krikidis, G. Zheng, and B. Ottersten, "Beamforming for MISO interference channels with QoS and RF energy transfer," *IEEE Transactions on Wireless Communications*, vol. 13, no. 5, pp. 2646–2658, 2014.
- [13] Q. Shi, L. Liu, W. Xu, and R. Zhang, "Joint transmit beamforming and receive power splitting for MISO SWIPT systems," *IEEE Transactions on Wireless Communications*, vol. 13, no. 6, pp. 3269–3280, 2014.
- [14] M. R. Khandaker and K.-K. Wong, "SWIPT in MISO multicasting systems," *IEEE Wireless Communications Letters*, vol. 3, no. 3, pp. 277–280, 2014.
- [15] S. Timotheou, G. Zheng, C. Masouros, and I. Krikidis, "Exploiting constructive interference for simultaneous wireless information and power transfer in multiuser downlink systems," *IEEE Journal on Selected Areas in Communications*, vol. 34, no. 5, pp. 1772–1784, 2016.
- [16] A. Özçelikkale and T. M. Duman, "Linear precoder design for simultaneous information and energy transfer over two-user MIMO interference channels," *IEEE Transactions on Wireless Communications*, vol. 14, no. 10, pp. 5836–5847, 2015.
- [17] J. Park and B. Clerckx, "Joint wireless information and energy transfer in a k -user MIMO interference channel," *IEEE Transactions on Wireless Communications*, vol. 13, no. 10, pp. 5781–5796, 2014.
- [18] X. Gui, Z. Zhu, and I. Lee, "Sum rate maximizing in a multi-user MIMO system with SWIPT," in *Proc. IEEE Vehicular Technology Conference (VTC Spring)*, July 2015, pp. 1–5.
- [19] Z. Zong, H. Feng, F. R. Yu, N. Zhao, T. Yang, and B. Hu, "Optimal transceiver design for SWIPT in k -user MIMO interference channels," *IEEE Transactions on Wireless Communications*, vol. 15, no. 1, pp. 430–445, 2016.
- [20] M.-M. Zhao, Y. Cai, Q. Shi, M. Hong, and B. Champagne, "Joint transceiver designs for full-duplex k -pair MIMO interference channel with SWIPT," *IEEE Transactions on Communications*, vol. 65, no. 2, pp. 890–905, 2017.
- [21] H. H. M. Tam, H. D. Tuan, A. A. Nasir, T. Q. Duong, and H. V. Poor, "MIMO energy harvesting in full-duplex multi-user networks," *IEEE Transactions on Wireless Communications*, vol. 16, no. 5, pp. 3282–3297, 2017.
- [22] S. Timotheou and I. Krikidis, "Joint information and energy transfer in the spatial domain with channel estimation error," in *Online Conference on Green Communications*, Feb. 2013, pp. 115–120.
- [23] S. Timotheou, I. Krikidis, S. Karachontzitis, and K. Berberidis, "Spatial domain simultaneous information and power transfer for MIMO channels," *IEEE Transactions on Wireless Communications*, vol. 14, no. 8, pp. 4115–4128, 2015.
- [24] S. Timotheou and I. Krikidis, "SWIPT through eigen-decomposition of MIMO channels," in *Proc. European Signal Processing Conference (EUSIPCO)*, Aug. 2015, pp. 1994–1998.
- [25] J. Tang, D. K. So, A. Shojaeifard, K.-K. Wong, and J. Wen, "Joint antenna selection and spatial switching for energy efficient MIMO SWIPT system," *IEEE Transactions on Wireless Communications*, vol. 16, no. 7, pp. 4754–4769, 2017.
- [26] D. Mishra and G. C. Alexandropoulos, "Jointly optimal spatial channel assignment and power allocation for MIMO SWIPT systems," *IEEE Wireless Communications Letters*, vol. 7, no. 2, pp. 214–217, 2018.
- [27] T. Le, K. Mayaram, and T. Fiez, "Efficient far-field radio frequency energy harvesting for passively powered sensor networks," *IEEE Journal of Solid-State Circuits*, vol. 43, no. 5, pp. 1287–1302, 2008.
- [28] J. Guo and X. Zhu, "An improved analytical model for RF-DC conversion efficiency in microwave rectifiers," in *IEEE/MTT-S International Microwave Symposium Digest*, June 2012, pp. 1–3.
- [29] C. R. Valenta and G. D. Durgin, "Harvesting wireless power: Survey of energy-harvester conversion efficiency in far-field, wireless power transfer systems," *IEEE Microwave Magazine*, vol. 15, no. 4, pp. 108–120, 2014.

- [30] E. Boshkovska, D. W. K. Ng, N. Zlatanov, and R. Schober, "Practical non-linear energy harvesting model and resource allocation for SWIPT systems," *IEEE Communications Letters*, vol. 19, no. 12, pp. 2082–2085, 2015.
- [31] E. Boshkovska, D. W. K. Ng, N. Zlatanov, A. Koelpin, and R. Schober, "Robust resource allocation for MIMO wireless powered communication networks based on a non-linear EH model," *IEEE Transactions on Communications*, vol. 65, no. 5, pp. 1984–1999, 2017.
- [32] K. Xiong, B. Wang, and K. R. Liu, "Rate-energy region of SWIPT for MIMO broadcasting under nonlinear energy harvesting model," *IEEE Transactions on Wireless Communications*, vol. 16, no. 8, pp. 5147–5161, 2017.
- [33] H. Niu, D. Guo, Y. Huang, and B. Zhang, "Robust energy efficiency optimization for secure MIMO SWIPT systems with non-linear EH model," *IEEE Communications Letters*, vol. 21, no. 12, pp. 2610–2613, 2017.
- [34] Y. Lu, K. Xiong, P. Fan, Z. Ding, Z. Zhong, and K. B. Letaief, "Global energy efficiency in secure MISO SWIPT systems with non-linear power-splitting EH model," *IEEE Journal on Selected Areas in Communications*, vol. 37, no. 1, pp. 216–232, 2019.
- [35] B. Clerckx and E. Bayguzina, "Waveform design for wireless power transfer," *IEEE Transactions on Signal Processing*, vol. 64, no. 23, pp. 6313–6328, 2016.
- [36] B. Clerckx, "Waveform optimization for SWIPT with nonlinear energy harvester modeling," in *Proc. International ITG Workshop on Smart Antennas (WSA)*, Mar. 2016, pp. 1–5.
- [37] M. Varasteh, B. Rassouli, and B. Clerckx, "Wireless information and power transfer over an AWGN channel: Nonlinearity and asymmetric Gaussian signaling," in *Proc. Information Theory Workshop (ITW)*, Nov. 2017, pp. 181–185.
- [38] M. Varasteh, B. Rassouli, H. Joudeh, and B. Clerckx, "SWIPT signalling over complex AWGN channels with two nonlinear energy harvester models," in *Proc. IEEE International Symposium on Information Theory (ISIT)*, June 2018, pp. 866–870.
- [39] R. Morsi, V. Jamali, D. W. K. Ng, and R. Schober, "On the capacity of SWIPT systems with a nonlinear energy harvesting circuit," in *Proc. IEEE International Conference on Communications (ICC)*, May 2018, pp. 1–7.
- [40] B. Clerckx, "Wireless information and power transfer: Nonlinearity, waveform design, and rate-energy tradeoff," *IEEE Transactions on Signal Processing*, vol. 66, no. 4, pp. 847–862, 2018.
- [41] B. Clerckx, R. Zhang, R. Schober, D. W. K. Ng, D. I. Kim, and H. V. Poor, "Fundamentals of wireless information and power transfer: From RF energy harvester models to signal and system designs," *IEEE Journal on Selected Areas in Communications*, vol. 37, no. 1, pp. 4–33, 2019.
- [42] Y. Jiang, W. Hager, and J. Li, "The generalized triangular decomposition," *Mathematics of computation*, vol. 77, no. 262, pp. 1037–1056, 2008.
- [43] Y. Jiang, J. Li, and W. W. Hager, "Uniform channel decomposition for MIMO communications," *IEEE Transactions on Signal Processing*, vol. 53, no. 11, pp. 4283–4294, 2005.
- [44] Y. Jiang, W. W. Hager, and J. Li, "Tunable channel decomposition for MIMO communications using channel state information," *IEEE Transactions on Signal Processing*, vol. 54, no. 11, pp. 4405–4418, 2006.
- [45] A. Al-Baidhani, M. Benaissa, and M. Vehkaperä, "Transceiver design for data rate maximization of MIMO SWIPT system based on generalized triangular decomposition," in *Proc. International Conference on Wireless Communications and Signal Processing (WCSP)*, Oct. 2018, pp. 1–5.
- [46] D. P. Palomar, Y. Jiang *et al.*, "MIMO transceiver design via majorization theory," *Foundations and Trends® in Communications and Information Theory*, vol. 3, no. 4-5, pp. 331–551, 2007.
- [47] K. Murata, N. Honma, K. Nishimori, and H. Morishita, "Analog eigenmode transmission for short-range MIMO," *IEEE Transactions on Vehicular Technology*, vol. 65, no. 1, pp. 100–109, 2016.
- [48] K. Murata, N. Honma, K. Nishimori, N. Michishita, and H. Morishita, "Analog eigenmode transmission for short-range MIMO based on orbital angular momentum," *IEEE Transactions on Antennas and Propagation*, vol. 65, no. 12, pp. 6687–6702, 2017.
- [49] P. Nintanavongsa, U. Muncuk, D. R. Lewis, and K. R. Chowdhury, "Design optimization and implementation for RF energy harvesting circuits," *IEEE Journal on Emerging and Selected Topics in Circuits and Systems*, vol. 2, no. 1, pp. 24–33, 2012.
- [50] G. Ma, J. Xu, Y. Zeng, and M. R. V. Moghadam, "A generic receiver architecture for MIMO wireless power transfer with non-linear energy harvesting," *IEEE Signal Processing Letters*, 2019.